⁄ ⁄ ⁄ ″K ›n

, ~ ‰ F ^ a ƒ ″ ƒ] ł ⁄ Dn ‹ O § @ ″ o › ‹ ¢ ‟ « ‰ Ł » P ⁄ ƒ ″ § › Pflf ' ¸ ⁄ « † z ´ ƒ ‡ ^ ¡ C ‟ ″ R fl ⁄ ‟ ‹ ‹ fl ⁄ f ¤ o ⁄ ' — ¯ ‚ ƒ ° ⁄ § A « ƒ ƒ „ ¡ A , ~ ‰ F ^ a ƒ ƒ] ⁄ l ' ¸ ‡ \ ´ ˙ … W ¥ [‟ ″ R fl ⁄ ƒ † › M ⁄ o ⁄ « ⁄ £ ª ‹ ¡ ¤ s § ¥ Dn ¥ ‟ ″ ⁄ D ƒ b ' — · Q , ~ ‰ F ^ a ƒ ″ ƒ] ⁄ l „ ‟ Rfl ⁄ § „ q ¥ ″ „ q ‹ y ¥ H ⁄ ¸ † › M ″ ¶ t ´ ⁄ l § @ ¥ ¸ ¡ C

⁄ Łk

´ ˙ ¥ † › M ″ ª ' w ¢ ¯ ¥ ¥ i O ¿ ¤ ‟ ″ R fl ⁄ ƒ † › M ¡ § B ° § @ „ q ‚ q ‹ y ¡ C ƒ † › M ⁄ ″ ¶ t ´ ⁄ l ¿ D ´ ¥ ¶ t › ¥ ¥ H · ¶ q ¡ A ¤ ^ æ , ‟ ″ R fl ⁄ ƒ † L › M ƒ ‡ — ¤ , ~ ‰ F ^ a ″ ƒ] ⁄ l ¡ ¥ ¥ { ⁄ § fi t § ¡ C

¶ G

‟ ″ R fl ⁄ ƒ † • › M › § „ ¢ † ƒ ‡ ‹ ƒ P ⁄ § ƒ ° , ‘ « ¡] 1.9±0.3 Hz ⁄ æ ⁄ W 1.8±0.3 Hz ¡ ^ A M ƒ ¡ A — ¤ , ~ ‰ F ^ a ƒ ″ ƒ] ⁄ l ⁄ § ‟ ‚ ƒ ⁄ § ƒ † § @ ƒ ‡ ¥ h • ¥ ˘ « ƒ (5.2±1.6 ⁄ æ ⁄ W 1.7±0.6 mV) ¡ C ‟ ″ R fl ⁄ ƒ ¤ † , › M ‰ F ^ a ″ ƒ] ⁄ l ¥ i ¥ H ¥ ¥ { , ß ⁄ p ⁄ § L « ‹ ¶ t ´ ⁄ l ‹ y ¡ A ƒ ƒ § … fi ' ° ¥ ~ ¥ „ [⁄ ‹ y ¡ B ' ° ⁄ l ⁄ ″ ‹ y ¥ ¶ ¶ t ¥ · « ´ ⁄ ‹ y ¡ A h ‟ ″ R fl ⁄ ƒ — † ¤ › M ~ ‰ F ^ a ƒ ″ ƒ] ⁄ ß l ¡ A ƒ ‡ ⁄ p ⁄ § ¶ t ´ ⁄ l ‹ y ¡ A , ß ⁄ p ⁄ § ƒ ‹ Y ¶ t ´ ⁄ l ¡ C

† ‰

, ~ ‰ F ^ a ″ ƒ] ⁄ W ¥ [‟ ″ R fl ⁄ ƒ ⁄ o ‡ ¤ « ⁄ ¶ G ¥ ¥ H ' ˜ ¡ A ¢ ƒ ¥ ⁄ ' — ¯ , ° ⁄ § f † z ´ ¡ C

^ ` : ‟ ″ R fl ¡ B , ~ ‰ F ^ a ″ ƒ] ⁄ l ¡ B „ q ¥ ″ † z

Abstract

Background: Tumor necrosis factor-α (TNF-α), a proinflammatory cytokine, has been implicated in the pathogenesis of cardiovascular diseases and cardiac arrhythmia. Pulmonary veins (PVs) were known to initiate paroxysmal atrial fibrillation. It is known that inflammation plays an important role in the genesis of atrial fibrillation. Therefore, it is possible that TNF-α may increase the PV arrhythmogenic activity to induce atrial fibrillation. The purpose of this study is to investigate the effects of TNF-α on PV electrophysiological characteristics, membrane currents and intracellular calcium. **Methods:** Whole-cell patch clamp were used to investigate the action potentials and ionic currents in isolated rabbit PV single cardiomyocytes with and without (control) incubation of 25 ng/ml TNF-α (6~ 12 hours). The intracellular calcium was measured through the indo 1 fluorimetric ratio technique in both groups. **Results:** There were similar spontaneous beating rates (1.9±0.3 Hz versus 1.8±0.3 Hz) between control (n=30) and TNF-α group (n=19). However, PV cardiomyocytes with TNF-α had larger amplitudes of delayed afterdepolarization than control cardiomyocytes (5.2±1.6 vs. 1.7±0.6 mV, $P<0.05$). TNF-α group has smaller L-type calcium currents, but has larger transient outward potassium, transient inward, and Na^{+}-Ca^{2+} exchanger than control group. TNF-α group has smaller intracellular calcium transient, smaller intracellular systolic calcium and longer decay potion of calcium transient (Tau). **Conclusions:** This study demonstrated that TNF-α increases PV arrhythmogenic activity, which may account for the genesis of inflammation related atrial fibrillation.

Key Words: pulmonary vein, Tumor necrosis factor-α, electrophysiology

Introduction

Tumor necrosis factor-α (TNF-α), is a proinflammatory cytokine that has been implicated in the pathogenesis of cardiovascular diseases, including heart failure, myocarditis, acute myocardial infarction and sepsis related cardiac dysfunction [1-6]. TNF-α also has been demonstrated to play a role in the genesis of cardiac arrhythmia. Mice with higher TNF-α expression has a greater incidence of atrial and ventricular arrhythmia [7]. Administration of TNF-α may induce arrhythmia with a loss of myocyte inotropy [8]. Additionally, previous studies have shown that TNF-α changes L-type calcium current and potassium current in ventricular myocytes [8-10]. All of these findings indicate the important role in the electrophysiology of cardiomyocytes. However, it is not clear whether TNF-α may also alter the electrophysiological characteristics of the cardiomyocytes with pacemaker activity. Moreover, knowledge about the arrhythmogenic mechanisms of TNF-α is limited.

Pulmonary veins (PVs) were known to be important sources of ectopic beats with the initiation of paroxysmal atrial fibrillation and the foci of ectopic atrial tachycardia. [11-13]. Other studies also suggested that PVs have a role in the maintenance of atrial fibrillation [14-15]. Previous anatomical and electrophysiological studies in isolated PV specimen have demonstrated that PVs contain a mixture of pacemaker cells and working myocardium; and were suggested to be subsidiary pacemaker to induce atrial arrhythmias. [16-19]. In addition, enhancement of automaticity and trigger activity was suggested to play a role in the high arrhythmogenic activity of PV cardiomyocytes with pacemaker activity [20-22]. Because inflammation plays an important role in the genesis of atrial fibrillation [23], it is possible that the inflammatory cytokine, TNF-α, may increase the arrhythmogenic activity of PV cardiomyocytes to induce atrial fibrillation. The purpose of this study is to investigate the effects of TNF-α on the electrical activity, intracellular calcium and membrane currents in PV cardiomyocytes with pacemaker activity.

Materials and Methods

Isolation of PV Cardiomyocytes

PV cardiomyocytes were enzymatically dissociated through the same procedure

described previously.[21] In brief, the heart with lungs were removed from anesthetized rabbits after mid-line thoracotomy. The PVs were perfused in a retrograde manner via a polyethylene tubing cannulated through the aorta and left ventricle into the left atrium. The free end of the polyethylene tube was connected to a Langendorff perfusion column for perfusion with oxygenated normal Tyrode's solution at 37°C (containing: NaCl 137, KCl 5.4, $CaCl_2$ 1.8, $MgCl_2$ 0.5, HEPES 10 and glucose 11 mM; the pH was adjusted to 7.4 by titrating with 1 N NaOH). The perfusate was replaced with oxygenated Ca^{2+}-free Tyrode's solution containing 300 units/ml collagenase (Sigma Type I) and 0.25 units/ ml protease (Sigma, Type XIV) for 8-12 min. The proximal PVs (8-12 mm) were cut away from the atrium and lung, and were gently shaken in 5-10 ml of Ca^{2+}-free oxygenated Tyrode's solution until single cardiomyocytes were obtained. The solution was then gradually changed to normal oxygenated Tyrode's solution. The cells were allowed to stabilize in the bath for at least 30 min before experiments.

Electrophysiological and pharmacological study

Whole-cell patch-clamp was performed in PV cardiomyocytes with and without the incubation of TNF-α (7-12 hours) by an Axopatch 1D amplifier (Axon Instruments, Calif, USA) at 35±1°C. Borosilicate glass electrodes (o.d., 1.8 mm) were used, with tip resistances of 3-5 MΩ. Before formation of the membrane-pipette seal, tip potentials were zeroed in Tyrode's solution. Junction potentials between the bath and pipette solution (9 mV) were corrected for AP recording. AP and membrane currents were measured during superfusion with normal Tyrode solution with (control group) or without TNF-α. The APs were recorded in current-clamp mode and ionic currents in voltage-clamp mode.[20-21] A small hyperpolarizing step from a holding potential of -50 mV to a testing potential of -55 mV for 80 ms was delivered at the beginning of each experiment. The area under the capacitative currents was divided by the applied voltage step to obtain the total cell capacitance. Normally, 60% to 80% series resistance (R_s) was electronically compensated. AP measurements were begun 5 minutes after cell rupture. In PV cardiomyocytes with spontaneous activity lesser than 1Hz, The AP duration at 20% (APD_{20}), 50% (APD_{50}) and 90% (APD_{90}) of full repolarization were measured during 1Hz electrical stimulation. The composition of pipette solution was as follows (in mM): KCl 20, K aspartate 110, $MgCl_2$ 1, Mg_2ATP 5,

HEPES 10, EGTA 0.5, LiGTP 0.1, and Na_2 phosphocreatine 5, adjusted to pH 7.2 with 1 N KOH. Voltage command pulses were generated by a 12-bit digital-to-analog converter controlled by pCLAMP software (Axon Instruments). Recordings were low pass-filtered at half the sampling frequency. Data were sampled at rates varying from 2 to 25 kHz.

Transient outward currents (I_{to}) were studied with a double-pulse protocol. A 30-ms pre-pulse from -80 to -40 mV was used to inactivate sodium channel, followed by a 300 ms test pulse to +60 mV in 10 mV steps at a frequency of 0.1 Hz. 200 μM $CdCl_2$ was added to the bath solution to inhibit $I_{Ca,L}$. I_{to} were measured as the difference between peak outward current and the outward current at the end of the test pulse. Delayed rectified outward potassium currents (I_K) were measured from the peak outward current at the end of 500 ms depolarization from -40 to +60 mV in 10 mV steps at a frequency of 0.1 Hz during the infusion of 200 μM $CdCl_2$ and 2 mM 4-aminopyridine in the bath solution to inhibit $I_{Ca,L}$ and I_{to}.

Transient inward current was induced at clamped potentials from -40 to +40 mV for the duration of 3 sec and then repolarized to -40 mV. The amplitude of transient inward current was measured as difference between the peak of the transient current and the mean of current just before and after the transient current.[20]

Hyperpolarization-activated membrane currents were activated from -40 mV to test potentials ranging from -20 to -120 mV in 10 mV steps for 1s at a frequency of 0.1 Hz under the infusion of 200 μM $CdCl_2$ and 2 mM 4-aminopyridine in the bath solution. The amplitudes of inward rectified potassium currents (I_{K1}) were measured as 1mM barium sensitive currents. Under the infusion of 1 mM barium to inhibit I_{K1}, a progressive large inward current developed with slow voltage-dependent kinetics was measured as pacemaker current (I_f) during hyperpolarization from a holding potential of -40 mV to a test potential of –120 mV for 1s.

For measurement of Na^+-Ca^{2+} exchanger (NCX) current, the external solution (in mM) was NaCl 140, $CaCl_2$ 2, $MgCl_2$ 1, HEPES 5 and glucose 10 with the pH adjusted to 7.4 and contained strophanthidin 10 μM (to block Na^+/K^+ pump), nitrendipine 10 μM (dihydropyrdine antagonist) and niflumic acid 100 μM (to block Ca^{2+} activated Cl^- currents). The pipette solution was as follows (in mM): NaCl 20, CsCl 110, $MgCl_2$ 0.4, $CaCl_2$ 1.75, tetraethylammonium 20, BAPTA 5, glucose 5, Mg_2ATP 5, HEPES 10 with

the PH adjusted to 7.25. The NCX current was elicited by depolarizing pulses between -80 to +100 mV from a holding potential of –40 mV. The amplitudes of NCX current were measured as 10 mM nickel-sensitive currents.

Measurement of Intracellular Ca

Intracellular Ca was recorded by a fluorimetric ratio technique (indo 1 fluorescence). The fluorescent indicator indo 1 was loaded by incubating the myocytes at room temperature for 10 to 12 minutes with 5μM of the acetoxymethyl ester form (indo 1-AM, Molecular Probes). PV cardiomyocytes were then perfused with normal bath solution at room temperature for at least 40 minutes to wash out extracellular indicator and to allow for intracellular deesterification of indo 1. Background and cell autofluorescence were cancelled out by zeroing the output of the photomultiplier tubes using cells without indo 1 loading. Ultraviolet light emanating from a mercury arc lamp was used to excite indo 1. Transmitted light was first split by a series of diachronic mirrors and passed through narrow-band-pass(+/- 10 nm) filters centered at 405 and 485 nm. Light intensity was monitored by means of 2 matched photomultiplier tubes (Hamamatsu type R2560HA). The analog ratio (Burr Brown Corp, model M/N DIV100HP) of the 2 fluorescent signals (405/485 nm) was electronically filtered with a low-pass Butterworth filter set at 60 Hz (Frequency Devices model 901) and digitized on line at 1 kHz by use of a computer-based acquisition system (TL-1-125 LabMaster Board, Axon Instruments Inc) and software (Axotape version 2.0, Axon Instruments Inc) to be stored on the computer's hard disk for later analysis and display. $R_{405/485}$ was used as the index of $[Ca^{2+}]_i$. This approach avoids uncertainties related to in vivo calibration of fluorescent Ca^{2+} indicators. The calcium transient, peak systolic calcium, diastolic calcium, and decay portion of calcium transient (τ_{Ca}) were measured during electrical stimulation (1.5 Hz, 3Hz, 6 Hz) in PV cardiomyocytes with spontaneous activity lesser than 1.5 Hz. τ_{Ca} were determinted by monoexpoential least-squares fit.

2.3. Statistics

Continuous variables are expressed as mean ± S.E.M. The differences among the PV cardiomyocytes with or without administration of TNF-α were analyzed by one-way ANOVA test. Multiple comparisons were analyzed with the Fisher LSD test. Nominal variables were compared by Chi-square analysis with Yates correction or

Fisher's exact test. A P value lower then 0.05 was considered to be statistically significant.

Results

Effect of TNF-α on the Electrical Activity of Single PV Cardiomyocytes

There were similar spontaneous beating rates, incidence of oscillatory potentials or delayed afterdepolarization (33%, 58%) in control and TNF-α group (Figure 1A). However, TNF-α-treated PV cardiomyocytes (n=10) had larger amplitudes (5.8±1.8 mV versus 2.6±0.8 mV) of delayed afterdepolarization than control (n=10) PV cardiomyocytes (Figure 1B).

During electrical stimulation, there were similar $\underline{APD_{90}}$ between control (n=12) and TNF-α (n=7) group (136±8 ms versus 127±11 ms, P>0.05). However, there is a shorter $\underline{APD_{20}}$ (58±6 ms versus 81±7 ms, P<0.05) and $\underline{APD_{50}}$ (30±5 ms versus 47±5 ms, P<0.05) in TNF-α group than in control Figure 1C shows the tracings of AP from the two groups.

Effect of TNF-α on Membrane Currents of PV Cardiomyocytes

There was smaller current density of $I_{Ca\text{-}L}$ in TNF-α group than in control. Figure 2 shows the tracings and I-V relationship of $I_{Ca\text{-}L}$ in the two groups. In contrast, as the examples show in Figure 3, the current density of I_{to} was larger in TNF-α group than in control. Moreover, there were similar current density of I_K between control and TNF-α group (Figure 4).

Figure 5 shows the recordings and I-V relationship of I_{K1} in TNF-α and control groups. There were similar current density of I_{K1} in the two groups. Additionally, there were similar I_f between control (n=8) and TNF-α (n=10) groups (0.24±0.06 pA/pF versus 0.38±0.09 pA/pF, P>0.05).

As the examples show in Figure 6, there were larger transient inward current (0.87±0.13 pA/pF vs. 0.48±0.08 pA/pF, P<0.01) in PV cardiomyocytes of TNF-α group (n=27) than in control group (n=16). Moreover, PV cardiomyocytes in TNF-α group have larger nickel-sensitive NCX currents than control group. Figure 7 shows the tracings and I-V relationship in both group.

Effect of TNF-α on Intracellular Calcium of PV Cardiomyocytes

As the examples show in Figure 8, TNF-α group (n=18) has smaller index of $[Ca^{2+}]_i$ transient (0.15±0.01 versus 0.22±0.01, P<0.0005), and similar index of peak

systolic $[Ca^{2+}]_i$ (0.82±0.02 versus 0.77±0.01, P>0.05) than control (n=13) group. However, TNF-α group has larger diastolic $[Ca^{2+}]_i$ (0.68±0.01 versus 0.55±0.01, P<0.0001) than control group. Moreover, TNF-α group had a longer decay portion of $[Ca^{2+}]_i$ transient than control group.

Discussion

Main Findings

This study showed that TNF-α increased delayed afterdepolarization, I_{to}, and I_{ti}, NCX currents, but decreased $I_{Ca\text{-}L.}$ TNF-α decreased the calcium transient, systolic calcium and decay potion of calcium transient (Tau) , but increased the diastolic calcium in PV cardiomyocytes.

Effects of TNF-α on Electrical Activity of PVs

In this study, we demonstrated that TNF-α may enhance the triggered activity of PV cardiomyocytes through an increase of delayed afterdepolarization. These findings confirmed that TNF-α plays a role in the arrhythmogenic activity of PVs. The proarrhythmogenic effects of TNF-α on PV cardiomyocytes may contribute to the higher incidences of atrial fibrillation during inflammation [23] and also may underline the genesis of atrial fibrillation after cardiac surgery [24-25]. Previous study has shown that congestive heart failure changes the atrial electrophysiology and results in a higher incidence of atrial fibrillation [26]. Because TNF-α is important to the progression of congestive heart failure [2, 3], the effects of TNF-α on PVs may also have a role in the genesis of atrial fibrillation during heart failure. In this study, we also demonstrated that TNF-α may shorten the $\underline{APD_{20}}$ and $\underline{APD_{50}}$. Previous studies have indicated that reentrant circuits in PVs may also have a role in PV arrhythmogenic activity [20, 27]. The shortening of $\underline{APD_{20}}$ and $\underline{APD_{50}}$ may facilitate the genesis of microreentrant and increase PV arrhythmogenic activity.

Effects of TNF-α on Membrane Currents of PV Cardiomyocytes

In this study, TNF-α was found to decrease $I_{Ca\text{-}L}$ in PV cardiomyocytes, which was similar to the known effects of TNF-α on ventricular myocytes. [8] The decrease of $I_{Ca\text{-}L}$ by TNF-α was suggested to contribute to the reduction of myocytes

contractility during sepsis and may also play a role in the TNF-α-induced reduction of calcium transient. Additionally, this study showed that TNF-α increase I_{to}, which may result in the shortening of $\underline{APD_{20}}$ and $\underline{APD_{50}}$. The similar current density of I_K and I_{K1} between control and TNF-α group may result in the similar resting membrane potential and $\underline{APD_{90}}$ in the two groups.

Previous studies have shown that I_f has a role in PV arrhythmogenic activity [21, 22]. However, it is not clear whether TNF-α may change I_f in PV cardiomyocytes. In this study, TNF-α was found to have little effects on I_f in PV cardiomyocytes. This result may contribute the similar PV automatic rhythm between control and TNF-α group.

I_{ti} is known to induce triggered activity and contribute to PV arrhythmogenic activity. [21, 22] In this study, we demonstrated that I_{ti} of PV cardiomyocytes were increased by TNF-α. In addition, we demonstrated that NCX currents were increased by TNF-α. NCX currents have been suggested to play a role in the genesis of I_{ti} and also contribute to delayed afterdepolarization in cardiomyocytes. These results suggested that TNF-α may alter NCX currents and then change the I_{ti} and arrhythmogenic activity of PV cardiomyocytes.

Effect of TNF-α on Intracellular Calcium of PV Cardiomyocytes

Although previous study has shown that TNF-α can decrease calcium transient and systolic calcium [4, 8, 9], it is not clear about the handling of intracellular calcium. In this study, we demonstrated than TNF-α can decreases $[Ca^{2+}]_i$ transient and peak systolic $[Ca^{2+}]_i$, but increase diastolic $[Ca^{2+}]_i$ in PV cardiomyocytes. This finding may result in the negative inotropic effects of TNF-α and contribute to the impaired heart function during sepsis. Moreover, for the first time, this study shows that there were longer $\underline{\tau_{Ca}}$ in TNF-α treated PV cardiomyocytes, which indicates that TNF-α slows the $[Ca^{2+}]_i$ reuptake. Because $[Ca^{2+}]_i$ decline arises from the function of NCX and SR Ca^{2+}-ATPase, the increase of NCX in TNF-α group indicated that the impaired decline of $[Ca^{2+}]_i$ is mainly caused by the impaired function of SR Ca^{2+}-ATPase. This result is similar to the known picture of heart failure with reduction of $[Ca^{2+}]_i$ transient, reduction of SR Ca^{2+}-ATPase and enhancement of NCX function [28]. Therefore, it is

possible that TNF-α play an import role to induce the electrophysiological changes during heart failure. Moreover, the impaired calcium reuptake of SR Ca^{2+}-ATPase by TNF-α may result in the increase of diastolic $[Ca^{2+}]_{i.}$ However, it is not clear whether the increase of TNF-α is caused by the direct effect of TNF-α or secondary to the increase of diastolic $[Ca^{2+}]_i$ and dysfunction of SR Ca^{2+}-ATPase.

Limitations

The limitation of this study is that we did not investigate the dose effects of TNF-α on PV cardiomyocytes. Additionally, the arrhythmogenic potentials of TNF-α may be underestimated because these cells were only incubated with TNF-α for 6 to 12 hours to maintain the viability of PV cardiomyocytes. Therefore, rather higher dosage (25 ng/ml) of TNF-α was used in this study

Conclusions

This study demonstrated that TNF-α increases PV arrhythmogenic activity, which may account for the higher incidence of atrial fibrillation in the patients during sepsis, post cardiac surgery, or with heart failure.

Acknowledgements

The present work was supported by grants NSC 92-2314-B010-052, NSC 92-2314-B075-117, NSC92-2314-B038-054, VGH92-238, VGH92-243, VTY 92-P5-34, VTY92-P5-29.

References

1. Latini R, Bianchi M, Correale E, et al. Cytokines in acute myocardial infarction: selective increase in circulating tumor necrosis factor, its soluble receptor, and interleukin 1 receptor antagonist. J Cardiovasc Pharmacol 1994;23:1-6.

2. Levine B, Kalman J, Mayer H, Fillit H, Packer M. Elevated circulating levels of tumor necrosis factor in severe chronic heart failure. N Engl J Med 190;323:236-241.

3. Packer M. Is tumor necrosis factor an important neurohormoral mechanism in chronic heart failure? Circulation 1995;92:1379-1382.

4. Yokoyama T, Vaca L, Rossen RD, et al. Cellular basis for the negative inotropic effects of tumor necrosis factor-a in the adult mammalian cardiac myocytes. J Clin Invest 1993;92:2303-2312

5. Kumar A, Thota V, Dee L, et al. Tumor necrosis factor-alpha and interleukin 1-beta are responsible for the in vitro myocardial cell depression induced by human septic shock serum. J Exp Med 1996 ;183 :949-958.

6. Low-Friedrich I, Weisensee D, Mitrou P, Schoeppe W. Cytokines induce stress protein formation in cultured cardiac myocytes. Basic Res Carddiol 1992 ;1 :12-18.

7. London B, Baker LC, Lee JS et al. Calcium-dependent arrhythmias in transgenic mice with heart failure. Am J Physiol 2002;284 :H431-H441.

8. Krown KA, Yasui Y, Brooker M, et al. TNFα receptor expression in rat cardiac myocytes : TNFα inhibition of L-type Ca^{2+} current and Ca^{2+} transients. FEBS Lett 1995 ;376 :24-30.

9. Goldhaber JI, Kim KH, Natterson PD. Effects of TNF-α on $[Ca^{2+}]i$ and contractility in isolated adult rabbit ventricular myocytes. Am J Physiol 1996;271:H1449-H1455.

10. Wang J, Wang H, Zhang Y, Gao H, Nattel S, Wang Z. Impairment of HERG K^+ channel function by tumor necrosis factor-α: role of reactive oxygen species as a mediator. J Biol Chem 2004;279:13289-13292.

11. Walsh EP, Saul JP, Hulse E, et al. Transcatheter ablation of ectopic atrial tachycardia in young patients using radiofrequency current. Circulation 1992;86:1138-1146.
12. Haissaguerre M, Jais P, Shah DC, et al. Spontaneous initiation of atrial fibrillation by ectopic beats originating in the pulmonary veins. N Engl J Med 1998;339:659-666.
13. Chen SA, Hsieh MH, Tai CT, et al. Initiation of atrial fibrillation by ectopic beats originating from the pulmonary veins: Electrophysiological characteristics, pharmacological responses, and effects of radiofrequency ablation. Circulation 1999;100:1879-1886.
14. Pappone C. Rosanio S. Oreto G. Tocchi M. Gugliotta F. Vicedomini G. Salvati A. Dicandia C. Mazzone P. Santinelli V. Gulletta S. Chierchia S. Circumferential radiofrequency ablation of pulmonary vein ostia: a new anatomic approach for curing atrial fibrillation. Circulation. 2000;102:2619-28
15. Sueda T, Imai K, Ishii O. Orihashi K, Watari M, Okada K. Efficacy of pulmonary vein isolation for the elimination of chronic atrial fibrillation in cardiac valvular surgery. Ann Thorac Surg 2001;71:1189-1193.
16. Masani F. Node-like cells in the myocardial layer of the pulmonary vein of rats: an ultrastructural study. J Anat 1986;145:133-142.
17. Perez-Lugones A, McMahon JT, Ratliff NB, Saliba WI, Schweikert RA, Marrouche NF, Saad EB, Navia JL, McCarthy PM, Tchou P, Gillinov AM, Natale A. Evidence of specialized conduction cells in human pulmonary veins of patients with atrial fibrillation. J Cardiovasc Electrophysiol. 2003;14:803-809.
18. Blom NA, Gittenberger-de Groot AC, DeRuiter MC, Poelmann RE, Mentink MM, Ottenkamp J. Development of the cardiac conduction tissue in human embryos using HNK-1 antigen expression: possible relevance for understanding of abnormal atrial automaticity. Circulation. 1999;99:800-806.
19. Cheung DW. Pulmonary vein as an ectopic focus in digitalis-induced arrhythmia. Nature 1981;294:582-584.
20. Chen YJ, Chen SA, Chang MS, Lin CI. Arrhythmogenic activity of cardiac muscle in pulmonary vein of the dog :Implication for the genesis of atrial Fibrillation. Cardiovasc Res 2000;48:265-273.

21. Chen YJ, Chen SA, Chen YC, Yeh HI, Paul C, Chang MS, Lin CI. Effects of rapid atrial pacing on the arrhythmogenic activity of single cardiomyocytes from pulmonary veins: implication in initiation of atrial fibrillation. Circulation 2001;2849-2854.
22. Chen YC, Chen SA, Chen YJ, Chang MS, Chan P, Lin CI. Effects of thyroid hormone on the arrhythmogenic activity of pulmonary vein cardiomyocytes. J Am Coll Cardiol. 2002;39:366-372.
23. Chung MK, Martin DO, Sprecher D, et al. C-reactive protein elevation in patients with atrial arrhythmias: inflammatory mechanisms and persistence of atrial fibrillation. Circulation 2001;104:2886-2891.
24. Zaman AG, Archbold RA, Helft G, Paul EA, Current NP, Mills PG. Atrial fibrillation after coronary artery bypass surgery: a model for preoperative risk stratification. Circulation 2000;101:1403-1408.
25. Mathew JP, Fontes Ml, Tudor IC, Ramsay J, Duke P, Mazer CD, Barash PG, Hsu PH, Mangano DT. A multicenter risk index for atrial fibrillation after cardiac surgery. JAMA 2004;291:1720-1729.
26. Li D, Melnyk P, Feng J, Wang Z, Petrecca K, **S**hrier A, Nattel S. Effects of Experimental Heart Failure on Atrial Cellular and Ionic Electrophysiology. Circulation 2000; 101: 2631 – 2638.
27. Hocini M, Ho SY, Kawara T, Linnenbank AC, Potse M, Shah D, Jais P, Janse MJ, Haissaguerre M, De Bakker JM**.** Electrical conduction in canine pulmonary veins: electrophysiological and anatomic correlation. Circulation. 2002;105:2442-2448.
28. Bers DM, Eisner DA, Valdiva HH. Sarcoplasmic Reticulum Ca^{2+} and Heart Failure: Roles of Diastolic Leak and Ca^{2+} Transport. Circ Res 2003;19:487-490.

Figure Legends

Figure 1. Action potentials of PV cardiomyocytes with and without administration TNF-α. Panel A. There were similar beating rates between control and TNF-α-treated PV cardiomyocytes. Panel B shows the larger delayed afterdepolarization (arrow) in TNF-α-treated than in control PV cardiomyocytes. Action potentials elicited by electrical stimulation are superimposed in control (▼) and TNF-α-treated (¡) PV cardiomyocytes. Panel C. There were shorter 20% and 50% of the AP duration in TNF-α-treated than in control PV cardiomyocytes. Action potentials elicited by electrical stimulation are superimposed in control (▼) and TNF-α-treated (¡) PV cardiomyocytes.

Figure 2. Effects of TNF-α on L-type calcium currents of PV cardiomyocytes Panel A shows the current traces L-type calcium currents in control and TNF-α-treated PV cardiomyocytes. Panel B shows the I-V relationship of L-type calcium currents in the two groups. There were smaller L-type calcium currents in TNF-α-treated (n= 7) than in control (n= 10) PV cardiomyocytes. Insets of current traces show the various clamp protocols. *P <0.05, versus control PV cardiomyocytes.

Figure 3. Effects of TNF-α on transient outward currents (I_{to}) of PV cardiomyocytes. Panel A shows the current traces of I_{to} in control and TNF-α-treated PV cardiomyocytes. Panel B shows the I-V relationship of I_{to} in the two groups. There were larger I_{to} in TNF-α-treated (n= 13) than in control (n= 10) PV cardiomyocytes. Insets of current traces show the various clamp protocols. *P <0.05, **P <0.01, ***P <0.005 versus control PV cardiomyocytes.

Figure 4. Effects of TNF-α on delayed rectified outward currents (I_K) of PV cardiomyocytes. Panel A shows the current traces of I_K in control and TNF-α-treated PV cardiomyocytes. Panel B shows the I-V relationship of I_K in the two groups. There were similar I_K between TNF-α-treated (n= 17) and control (n= 14) PV cardiomyocytes. Insets of current traces show the various clamp protocols.

Figure 5. Effects of TNF-α on inward rectified potassium currents (I_{K1}) of PV cardiomyocytes. Panel A shows the current traces of I_{K1} in control and TNF-α-treated PV cardiomyocytes. Panel B shows the I-V relationship of I_{K1} in the two groups. There were similar I_{K1} between TNF-α-treated (n= 10) and control (n= 8) PV cardiomyocytes. Insets of current traces show the various clamp protocols.

Figure 6. Effects of TNF-α on transient inward currents of PV cardiomyocytes. Panel A shows the larger transient inward current (¡) in TNF-α-treated than in control PV cardiomyocytes. Insets of current traces show the clamp protocols.

Figure 7. Effects of TNF-α on Na^{+}-Ca^{2+} exchanger (NCX) currents in PV cardiomyocytes. Panel A shows the current traces of NCX in control and TNF-α-treated PV cardiomyocytes. Panel B shows the I-V relationship of NCX currents in the two groups. There were larger NCX currents in TNF-α-treated (n= 11) than in control (n= 12) PV cardiomyocytes. Insets of current traces show the various clamp protocols. *P <0.05, **P <0.01, ***P <0.005 versus control PV cardiomyocytes.

Figure 8. Effects of TNF-α on intracellular calcium of PV cardiomyocytes. Panel A shows the superimposed calcium transient in control (▼) and TNF-α-treated (¡) PV cardiomyocytes.

Fig 1.

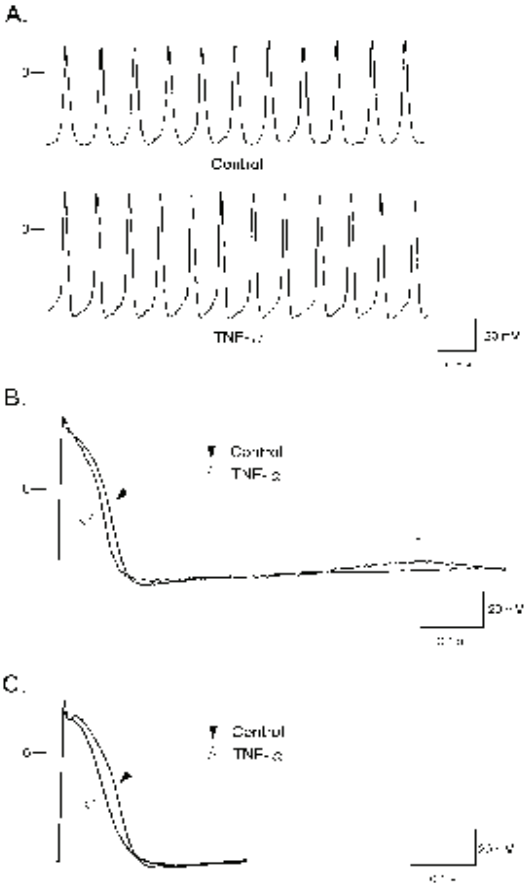

Fig 2.

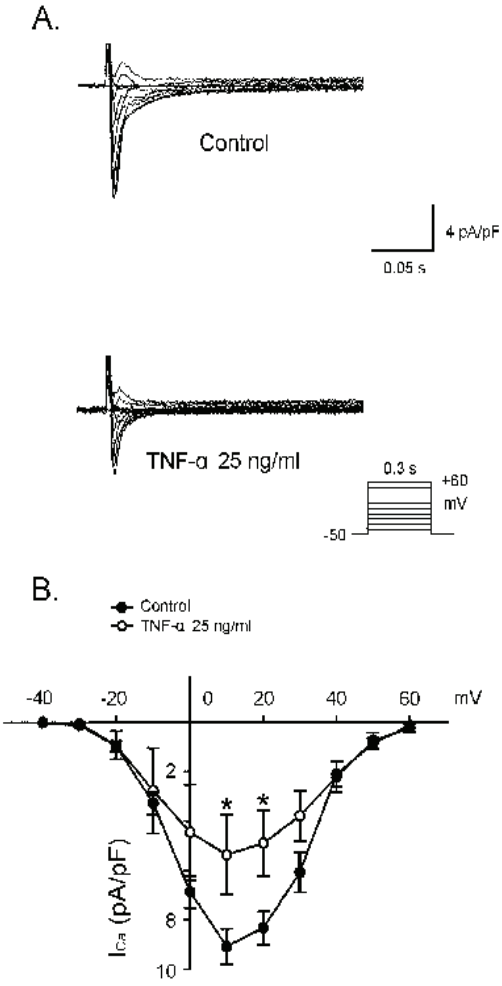
A.
Control
4 pA/pF
0.05 s
TNF-α 25 ng/ml
0.3 s
+60
mV
-50
B.
Control
TNF-α 25 ng/ml
-40
-20
0
20
40
60
mV
2
8
10
I_{Ca} (pA/pF)
*
*

Fig 3.

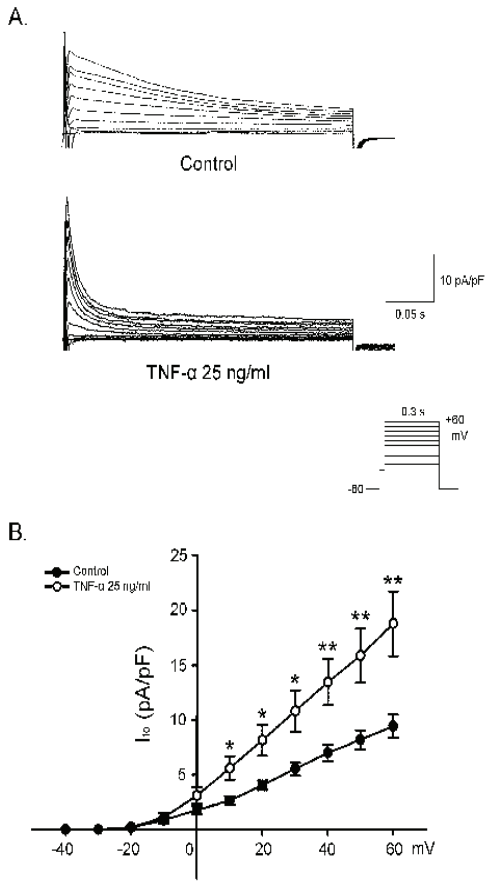
A.
Control
10 pA/pF
0.05 s
TNF-α 25 ng/ml
0.3 s
+60 mV
-80
B.
Control
TNF-α 25 ng/ml
I_{to} (pA/pF)
25
20
15
10
5
-40
-20
0
20
40
60 mV
*
**

Fig 4.

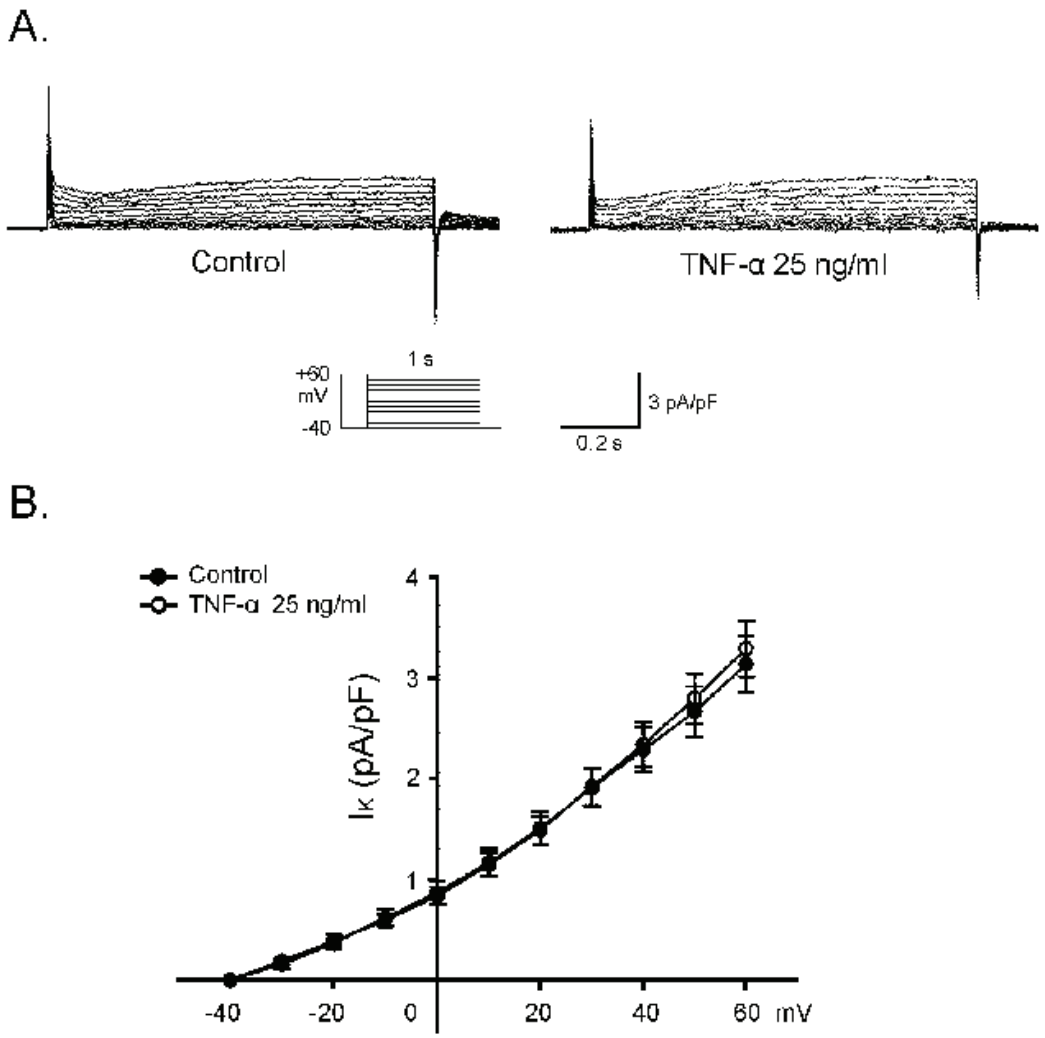
A.
Control
TNF-α 25 ng/ml
1 s
+60
mV
-40
3 pA/pF
0.2 s
B.
Control
TNF-α 25 ng/ml
Ik (pA/pF)
4
3
2
1
-40
-20
0
20
40
60 mV

Fig 5.

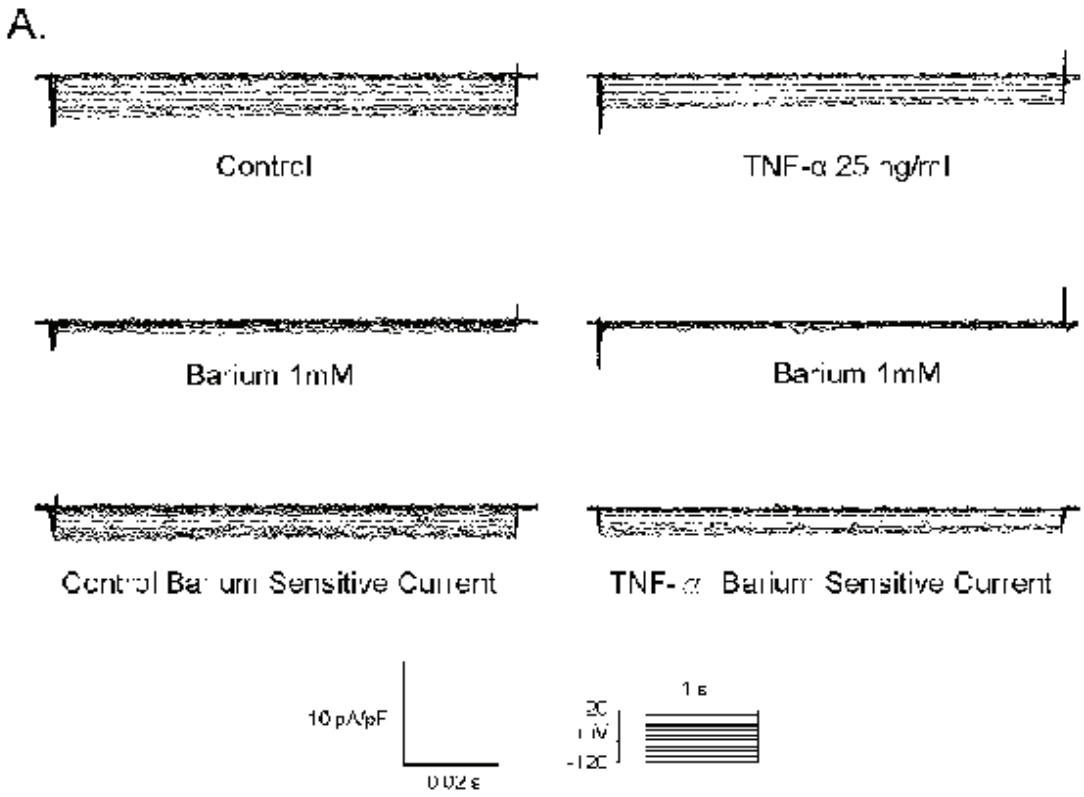
A.
Control
TNF-α 25 ng/ml
Barium 1mM
Barium 1mM
Control Barium Sensitive Current
TNF-α Barium Sensitive Current
10 pA/pF
0.02 s
1 s
20
-120
B.
Control
TNF-α 25 ng/ml
mV
120
-40
0
-1
-2
-3
-4
(pA/pF)

Fig 6.

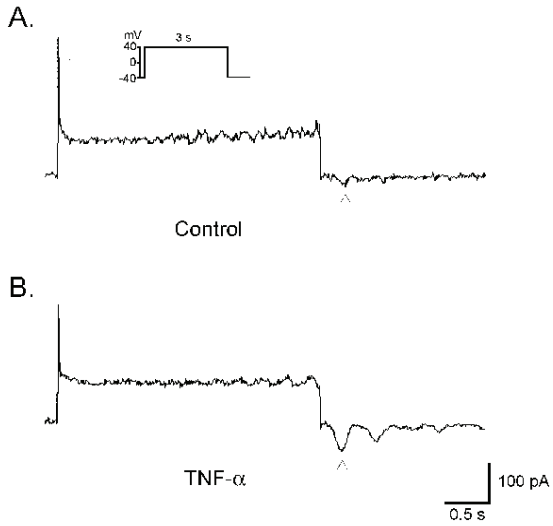

Fig 7.

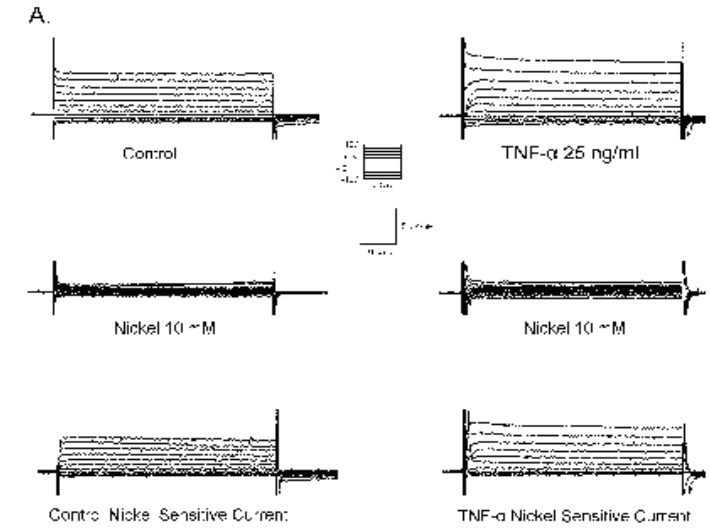
A.
Control
TNF-α 25 ng/ml
Nickel 10 mM
Nickel 10 mM
Contro Nicke Sensitive Curren
TNF-α Nickel Sensitive Current

B.

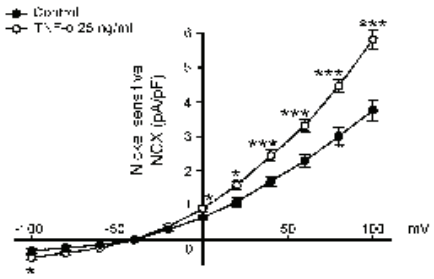
Control
TNF-α 25 ng/ml
Nicka sensitiva
NCX (pA/pF)
mV
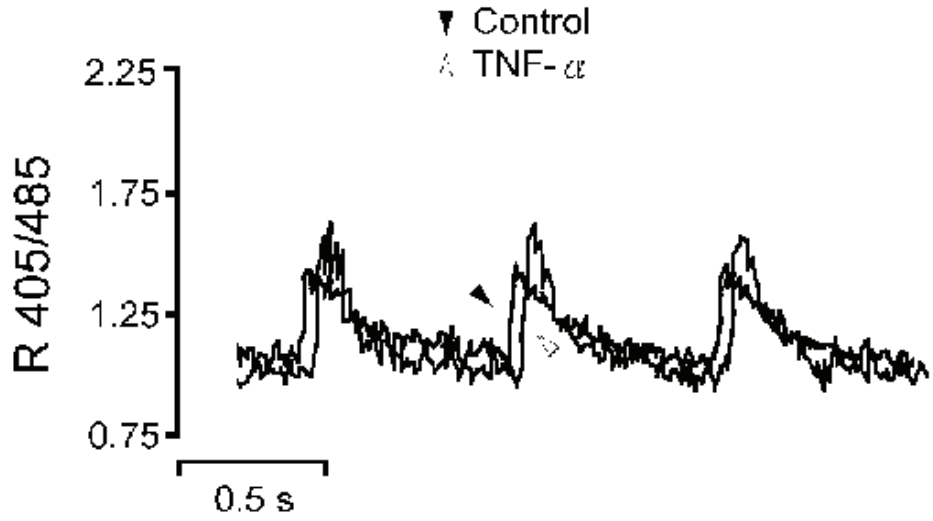
Fig 8.